

An Optical Thermometer Based on the Delayed Fluorescence of C₇₀

Carlos Baleizão,^[a] Stefan Nagl,^[b] Sergey M. Borisov,^[b] Michael Schäferling,^[b]
Otto S. Wolfbeis,^[b] and Mário N. Berberan-Santos^{*[a]}

Abstract: A sensitive and broad-ranged optical thermometer, based on the thermally activated delayed fluorescence of fullerene C₇₀, is presented. It consists of C₇₀ molecularly dispersed in a polymer film. Several polymer matrices were investigated. In the absence of oxygen the fluorescence intensity increases markedly with temperature. At 25 °C the fluorescence intensity of C₇₀ increases maximally by a factor of between 17 and 22, depending on the polymer, whereas at 100 °C the fluorescence intensity can be 79 times higher. In the absence of oxygen and for tem-

peratures above 20 °C, the red fluorescence of C₇₀ in the films is so intense that it is easily perceived by the naked eye. For the systems studied, the fluorescence intensity is very sensitive to temperature. This results in a working range from -80 to at least 140 °C in the case of C₇₀ in poly(*tert*-butyl methacrylate) (PtBMA). Perylene was incorporated into the film as an internal

Keywords: C₇₀ • fluorescence • fullerenes • imaging • sensors • temperature sensing

reference in order to enable ratiometric measurements. The sensitivity of the lifetime of the delayed fluorescence to temperature is also high and results in an even wider working range. The performance of the C₇₀/PtBMA film was measured against a well-known optical temperature probe, [Ru(phen)₃] (phen = phenanthroline). The results show that the C₇₀/PtBMA film is a very good system for optical temperature-sensing over a wide range of temperatures, outperforming known standards.

Introduction

Temperature is a basic physical parameter, and its measurement is often required both in scientific research and in industrial applications. Real-time temperature monitoring is of paramount importance in industrial testing and manufacturing and also in many biomedical diagnostic and treatment processes. Among the many optical methods which are employed for sensing, luminescence has attracted special attention because it is sensitive, versatile, and can be used even in very strong electromagnetic fields which are employed, for example, in hyperthermal cancer therapy.^[1] Given that luminescence can be both excited and measured optically, luminescence-based remote temperature sensors have ad-

vantages over contact temperature sensors in applications where electromagnetic noise is strong or it is physically difficult to connect a wire as there is no contact with the medium in the sensing process.^[2-4] Furthermore, temperature imaging using planar sensors is easily achieved in this way. Additional advantages of a luminescence-based thermometer are the usually fast response and the spatial resolution that can extend from the macroscale (in the case of luminescent paints) down to the nanoscale (such as in fluorescence microscopy).

Whereas virtually any intra- or intermolecular temperature-dependent process that affects the photophysical properties of a luminophore (spectrum, intensity, lifetime, polarization) can in principle be used for the design of a molecular thermometer, all available working luminescence thermometers are based on inorganic solids or organic molecules incorporated into solid-state matrices, including polymer particles and films. In these systems, the decay times and intensities almost invariably decrease with an increase in temperature owing to thermally activated quenching processes.^[4-9]

The common mechanism of molecular fluorescence^[10] is prompt fluorescence (PF) in which emission occurs after S_n ← S₀ absorption and excited-state relaxation to S₁. A

[a] Dr. C. Baleizão, Prof. Dr. M. N. Berberan-Santos
Centro de Química-Física Molecular
Instituto Superior Técnico, 1049-001 Lisboa (Portugal)
Fax: (+351)218-464-455
E-mail: berberan@ist.utl.pt

[b] Dipl.-Chem. S. Nagl, Dr. S. M. Borisov, Dr. M. Schäferling,
Prof. Dr. O. S. Wolfbeis
Institute of Analytical Chemistry, Chemo- and Biosensors
University of Regensburg, 93040 Regensburg (Germany)

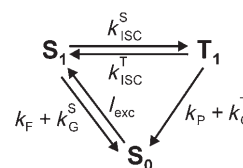
second, much less common, unimolecular mechanism is thermally activated delayed fluorescence (TADF)^[10] in which, after excitation to the first excited singlet state (S_1), intersystem crossing to the triplet manifold (triplet state T_1) occurs followed by a second intersystem crossing back to S_1 . The cycle may be repeated a number of times before fluorescence finally takes place. TADF is significant only if the S_1 – T_1 energy gap (ΔE_{ST}) is small and if the lifetime of T_1 is long enough. Despite being known for a long time, TADF continues to be a rare and usually weak phenomenon; there have been just a few observations in xanthenes dyes,^[10] aromatic ketones,^[11,12] thiones,^[13] and aromatic hydrocarbons.^[14–16] Probably for this reason TADF has not been used before for temperature measurement, with one single, but interesting exception. Harris and co-workers^[17] proposed the use of the known delayed fluorescence of Acridine Yellow for the development of a molecular thermometer in the -50 to $+50^\circ\text{C}$ range. However, the TADF of this compound is very weak, which precludes fluorescence intensity measurements without the use of a time delay. Furthermore, the observed triplet decay is complex, preventing a clear interpretation of the results.

Fullerene C_{70} has unique photophysical properties: its quantum yield for triplet formation is close to one, its ΔE_{ST} is quite small, and its intrinsic triplet lifetime is in the order of several milliseconds.^[18–20] This led to the discovery^[21] that C_{70} has an exceptionally intense TADF. There is presently a need for sensors covering a wide temperature range, and we perceived that C_{70} is well-suited for this purpose given that the fluorescence intensity of C_{70} increases markedly with temperature between -80 and at least 140°C and that the TADF lifetime decreases markedly with temperature between -50°C and an estimated upper limit of at least 450°C (as described in this work). Apart from a strong TADF, C_{70} exhibits good photostability and has high molar absorption (e.g., $2 \times 10^4 \text{ M}^{-1} \text{ cm}^{-1}$ at 470 nm). Note that other fullerenes, for example, a C_{70} derivative,^[22] fullerene C_{60} ,^[23] and some C_{60} derivatives,^[24,25] also exhibit TADF, but in all these cases it is much weaker than that of C_{70} .

We describe herein a new type of polymer thermometer whose function is based on the delayed fluorescence of C_{70} .^[26] These thermometers cover a broad range of temperature, encompassing the important physiological interval. Several polymers have been used as matrices for C_{70} . Temperature-dependent imaging of the C_{70} films was carried out using both steady-state and lifetime methods. In the presence of oxygen, the fluorescence intensity of the C_{70} film is essentially temperature-independent. However, in its absence, the fluorescence intensity increases markedly with temperature. At room temperature (25°C), and after degassing the sample, the fluorescence intensity of C_{70} increases with temperature maximally by a factor of 22, depending on the polymer, while at 100°C , the fluorescence intensity can be 79 times higher. The systems studied cover a working range from -80 to at least 140°C .

Results and Discussion

Thermally activated delayed fluorescence kinetics: The kinetics of thermally activated delayed fluorescence can be represented by Scheme 1, where I_{exc} is the excitation intensity, k_F and k_p are the radiative rate constants for fluorescence and phosphorescence, respectively, k_G^S and k_G^T are the nonradiative rate constants for deactivation to the ground state (internal conversion from S_1 and intersystem crossing from T_1 , respectively), and k_{ISC}^S and k_{ISC}^T are the intersystem crossing rate constants for singlet-to-triplet and triplet-to-singlet conversion, respectively. The rate constant k_{ISC}^T corresponds to an activated process and is strongly temperature-dependent [Eq. (1), where ΔE_{ST} is the S_1 – T_1 energy gap].^[21,27,28]



Scheme 1. Kinetic scheme for TADF.

$$k_{\text{ISC}}^T = A \exp\left(-\frac{\Delta E_{ST}}{RT}\right) \quad (1)$$

For strong TADF to occur, the following inequalities need to be met: $k_{\text{ISC}}^S \gg k_F + k_G^S$ and $k_{\text{ISC}}^T \gg k_p + k_G^T$. In most cases $k_{\text{ISC}}^S \gg k_{\text{ISC}}^T$ and $k_G^T \gg k_p$ are also observed. Interconversion of the singlet and triplet emissive states occurs many times before photon emission or nonradiative decay can take place. In this way, a fast pre-equilibrium between S_1 and T_1 exists, and for a sufficiently long time both S_1 and T_1 decay with a common rate constant, given by Equation (2).^[29]

$$k = \frac{k_{\text{ISC}}^S}{k_{\text{ISC}}^S + k_{\text{ISC}}^T} k_G^T + \frac{k_{\text{ISC}}^T}{k_{\text{ISC}}^S + k_{\text{ISC}}^T} k_G^S \quad (2)$$

Given the inequalities mentioned above, Equation (2) simplifies to Equation (3), where Φ_T is the quantum yield for triplet formation, $\Phi_T = k_{\text{ISC}}^S / (k_F + k_G^S + k_{\text{ISC}}^S)$, and τ_{DF} is the delayed fluorescence (and phosphorescence) lifetime. From Equation (1) and Equation (3), Equation (4) can be obtained, where $B = (1 - \Phi_T)A$. From a fit to the temperature dependence of the delayed fluorescence lifetime using Equation (4) and by assuming that k_G^T is temperature-independent, it is possible to determine ΔE_{ST} , B , and k_G^T .

$$k = \frac{1}{\tau_{\text{DF}}} = k_G^T + (1 - \Phi_T)k_{\text{ISC}}^T \quad (3)$$

$$\frac{1}{\tau_{\text{DF}}} = k_G^T + B \exp\left(-\frac{\Delta E_{ST}}{RT}\right) \quad (4)$$

The fluorescence quantum yield is given by Equation (5), where the quantum yields for prompt Φ_{PF} and delayed Φ_{DF} fluorescence obey the relation given by Equation (6)^[21] and the quantum yield for singlet formation is defined by Equation (7).

$$\Phi_F = \Phi_{PF} + \Phi_{DF} \quad (5)$$

$$\frac{\Phi_{DF}}{\Phi_{PF}} = \frac{I_{DF}}{I_{PF}} = \frac{1}{\frac{1}{\Phi_S \Phi_T} - 1} \quad (6)$$

$$\Phi_S = \frac{k_{ISC}^T}{k_p + k_G^T + k_{ISC}^T} \quad (7)$$

In the high-temperature limit, $k_{ISC}^S \gg k_p + k_G^T$. Hence, $\Phi_S = \Phi_S^\infty = (A/(k_p + k_G^T + A)) = 1$ (assuming that even in this range $A \gg k_G^T$) and Equation (6) becomes Equation (8).

$$\left(\frac{\Phi_{DF}}{\Phi_{PF}}\right)_{\max} = \left(\frac{I_{DF}}{I_{PF}}\right)_{\max} = \frac{1}{\Phi_T - 1} \quad (8)$$

For the purpose of curve fitting, Equation (6) can be conveniently rewritten as Equation (9),^[21] and from a fit to this expression it is possible to determine ΔE_{ST} , Φ_T , and Φ_S^∞ . By combining steady-state and time-resolved data, it is in principle possible to calculate ΔE_{ST} , Φ_T , Φ_S^∞ , A , and k_G^T .

$$\ln \left[\frac{I_{DF}}{I_{PF}} - \left(\frac{1}{\Phi_T} - 1 \right) \right] = \ln \left[\frac{1}{\Phi_T} \left(\frac{1}{\Phi_S^\infty} - 1 \right) \right] + \frac{\Delta E_{ST}}{RT} \quad (9)$$

C₇₀ delayed fluorescence: general aspects and polymer matrix effects:

To evaluate the influence of the polymer matrix structure on the photophysics and TADF of C₇₀, three polymers were selected: Polystyrene (PS), poly(*tert*-butyl methacrylate) (PtBMA), and poly(1-vinylnaphthalene) (P1VN). The films were prepared by evaporating a toluene solution of C₇₀ and the polymer deposited on a quartz plate. After film formation and drying, the plates were placed in a quartz cell that was degassed at room temperature and afterwards sealed. All the films exhibited absorption spectra similar to that of C₇₀ in toluene (for PS and P1VN) or methylcyclohexane (for PtBMA). These results are in agreement with a molecular dispersion of C₇₀ in the polymeric films.

The fluorescence of the C₇₀/PS film at different temperatures and over a full heating-cooling cycle is shown in Figure 1. The first spectrum was recorded at room temperature (25 °C) before degassing and corresponds to prompt fluorescence (PF). Without degassing, the fluorescence intensity is temperature-independent. After degassing, a 22-fold enhancement of the room-temperature fluorescence was observed. This enhancement is a consequence of the additional contribution of delayed fluorescence (DF) to the overall emission. Heating of the sample to 100 °C (Figure 1a) (a temperature at which the DF is 70 times higher than the PF) shows that the fluorescence of C₇₀ has a strong temperature dependence. The C₇₀/PS film exhibits full reversibility and fluorescence intensity cycles without hysteresis. The experiment was repeated three times and exhibited a high degree of reproducibility.

The values of I_{DF}/I_{PF} for the C₇₀/PS film at different temperatures are collected in Table 1, and compared with the values previously measured for a solution of C₇₀ in liquid paraffin.^[21] The I_{DF}/I_{PF} ratios for the C₇₀/PS film are always

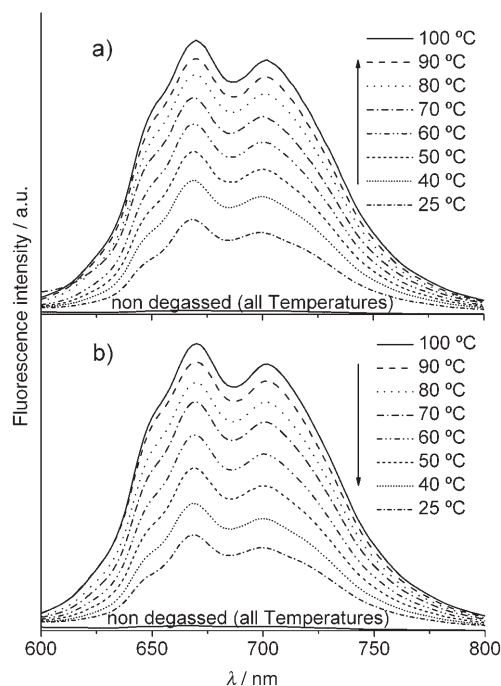


Figure 1. Fluorescence spectra ($\lambda_{exc} = 470$ nm) of a degassed C₇₀/PS film at different temperatures: a) heating cycle (from 25 to 100 °C); b) cooling cycle (from 100 to 25 °C). The emission of the non-degassed sample is also shown for comparison.

Table 1. Experimental I_{DF}/I_{PF} values (700 nm) for the C₇₀/polymer systems at various temperatures.

System	I_{DF}/I_{PF} (700 nm)			
	25 °C	50 °C	70 °C	100 °C
C ₇₀ /paraffin ^[a]	20	35	50	–
C ₇₀ /PS	22	39	53	70
C ₇₀ /P1VN	17	30	40	50
C ₇₀ /PtBMA	18	35	51	79

[a] See reference [21].

higher than the values reported for C₇₀ in paraffin. The values of I_{DF}/I_{PF} for the films were also measured over a wider temperature range than for C₇₀ in paraffin. The stability of the C₇₀/PS after long-term storage is also high, with comparable ratios (less than 2% variation) of I_{DF}/I_{PF} being measured after several weeks of storage.

Identical temperature cycles were carried out for the C₇₀/P1VN and C₇₀/PtBMA films. Responses similar to that of the C₇₀/PS film were observed. The films exhibit very good reversibility in the thermal cycles and high reproducibility. The I_{DF}/I_{PF} values for these films at several temperatures are also reported in Table 1. The maximum I_{DF}/I_{PF} value was obtained at 100 °C with the C₇₀/PtBMA system.

From an analysis of the delayed fluorescence data using the method previously developed^[21] it is possible to obtain ΔE_{ST} from the temperature dependence of the I_{DF}/I_{PF} ratio. However, the correct value of Φ_T (assumed to be temperature-independent) is required for a linear least-squares fit. The shape of the plot is very sensitive to Φ_T and is in gener-

al nonlinear (Figure 2). Variation of this parameter in the search for maximum linearity yields its best value and, simultaneously, ΔE_{ST} and clearly demonstrates the extreme sensitivity to Φ_T in the high temperature domain. Figure 2 shows that the value of Φ_T determined in this way is quite precise.

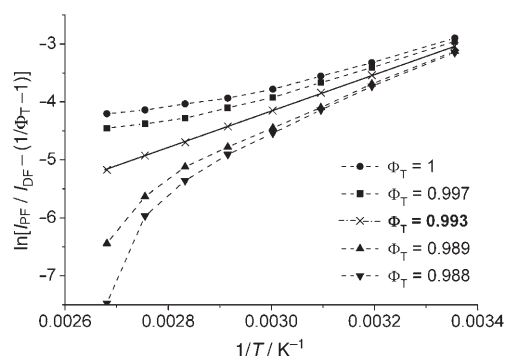


Figure 2. Fit of $\ln[I_{DF}/I_{PF} - (1/\Phi_T - 1)]$ versus $1/T$ according to Equation (9) for the C_{70} /PtBMA film in the temperature range of 25–100 °C. The best straight line ($r^2 = 0.999$) is obtained for $\Phi_T = 0.993$.

By using this method, it was possible to obtain for C_{70} /PtBMA a value for Φ_T of 0.993 and an effective singlet–triplet energy gap of 26 kJ mol⁻¹, both in good agreement with the values determined for C_{70} in paraffin (0.994 and 26 kJ mol⁻¹, respectively). From the experimental value, $\Phi_T = 0.993$, and from Equation (7), one finds for the high-temperature limit that $(I_{DF}/I_{PF})_{max} = 142$. In this way, the global fluorescence quantum yield ($\Phi_F = \Phi_{PF} + \Phi_{DF}$) of C_{70} in PtBMA film can be maximally 143 times higher than that of prompt fluorescence and thus attain the significant value of $143 \times (5 \times 10^{-4}) = 0.071$. These calculations were also carried out for the other two polymer systems and the results are given in Table 2, along with those for the C_{70} /paraffin

Table 2. Photophysical parameters for C_{70} in the three polymers and in liquid paraffin.

System	Φ_T	ΔE_{ST} [kJ mol ⁻¹]	Φ_F^{max}	$-\log \Phi_S^\infty [10^{-7}]$	$\tau_{PF}^{[a]}$ [ns]	$\tau_{DF}^{[a]}$ [ms]
C_{70} /paraffin ^[b]	0.994	26	0.080	–	0.65	36
C_{70} /PS	0.989	29	0.046	1.285	0.63	21
C_{70} /P1VN	0.986	27	0.036	2.688	0.60	20
C_{70} /PtBMA	0.993	26	0.071	5.663	0.62	27

[a] At 25 °C. [b] See reference [21].

system. The prompt fluorescence lifetime τ_{PF} at room temperature was also measured for all the systems (0.60–0.63 ns) and the values are very similar to the value for C_{70} /paraffin (0.65 ns).

The experimental and fitted values of I_{DF}/I_{PF} as a function of temperature are presented in Figure 3, with the fitting

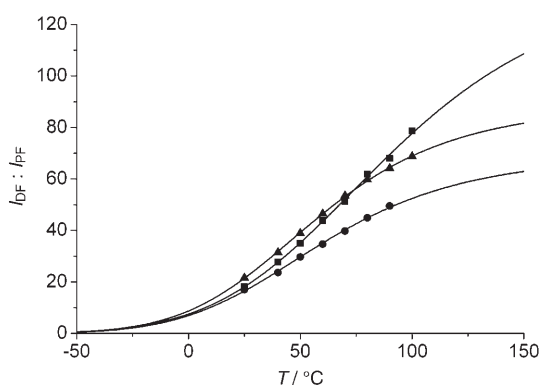


Figure 3. Plot of experimental and calculated (solid lines) I_{DF}/I_{PF} values (700 nm) versus temperature, according to Equation (10) for C_{70} /PtBMA (squares), C_{70} /PS (triangles), and C_{70} /P1VN (circles).

being made to Equation (10) and also Equation (11), Equation (12), and Equation (13).

$$\frac{I_{DF}}{I_{PF}} = (a + be^{c/T})^{-1} \quad (10)$$

$$a = \frac{1}{\Phi_T} - 1 \quad (11)$$

$$b = \frac{1}{\Phi_T} \left(\frac{1}{\Phi_S^\infty} - 1 \right) \quad (12)$$

$$c = \frac{\Delta E_{ST}}{R} \quad (13)$$

As can be seen from Figure 3, the fit is quite good. Although the maximum experimental temperature was 100 °C, it is in principle possible to go to higher temperatures and further increase the I_{DF}/I_{PF} ratio.

The three systems have an identical I_{DF}/I_{PF} response for temperatures less than 40 °C. Above this temperature, the curves start to diverge, as can be seen in Figure 3. The C_{70} /P1VN system attains an extrapolated $(I_{DF}/I_{PF})_{max}$ of 70, whereas C_{70} /PS reaches an extrapolated $(I_{DF}/I_{PF})_{max}$ value of 90. With the C_{70} /PtBMA system it is possible in principle to obtain a value for $(I_{DF}/I_{PF})_{max}$ of 142. Clearly, this is the system that displays the best photophysical properties for temperature-sensing at higher temperatures. An explanation for the superior photophysical properties of the C_{70} /PtBMA system (see Table 2) lies in the inertness of the backbone of PtBMA to possible quenching interactions with C_{70} . Weak π – π interactions between the fullerene and the phenyl rings^[30] of the backbone of P1VN and PS are the likely reason for the lower efficiency of these systems.

Temperature sensitivity of fluorescence intensity: The temperature sensitivity of fluorescence intensity can be defined either as the variation of the fluorescence quantum yield with temperature, which is the absolute sensitivity S_A [Eq. (14)], or as the relative variation of the fluorescence

quantum yield with temperature, which is the relative sensitivity S_R [Eq. (15)].

$$S_A = \frac{d\Phi_F}{dT} \quad (14)$$

$$S_R = \frac{1}{\Phi_F} \frac{d\Phi_F}{dT} = \frac{d \ln \Phi_F}{dT} \quad (15)$$

We will use the relative sensitivity as it directly reflects the relative variation of the fluorescence intensity. The temperature dependence of S_R for the C₇₀/polymer systems is displayed in Figure 4. It can be seen that the C₇₀/polymer

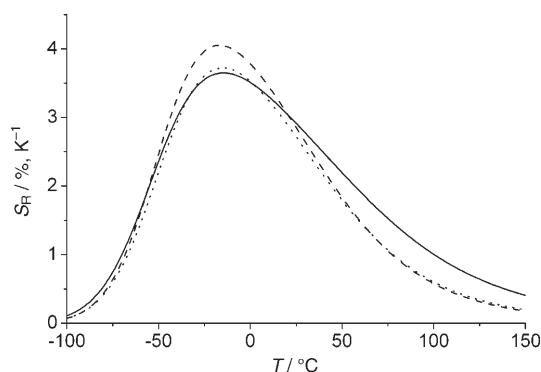


Figure 4. Relative variation S_R in fluorescence versus temperature for C₇₀/PtBMA (solid line), C₇₀/PS (dashed line), and C₇₀/P1VN (dotted line).

systems have some of the highest temperature sensitivities known over a broad temperature range.^[2]

In order to be useful in practice, a minimum value of 0.5% K⁻¹ for S_R is assumed. With this value, the lower temperature limit is -80°C for all polymers. At the other end of the scale, the C₇₀/PtBMA system displays the highest high-temperature limit (140°C), whereas for the other two polymers the upper limit is 110°C. Note that the lower and upper temperature values found may not be the real ones because, whilst a condition such as $S_R > 0.5\% \text{ K}^{-1}$ is necessary, it is not necessarily a satisfactory one. In fact, an arbitrarily small value for the absolute intensity cannot be set owing to background noise, and this aspect is best evaluated from the temperature dependence of the fluorescence quantum yield (Figure 5). It can be seen that this dependence may somewhat increase the lower temperature limits found, -80°C, but will not change the estimated upper temperature limits.

Delayed fluorescence lifetime: The delayed fluorescence lifetimes (τ_{DF}) of all the systems were determined for the temperature range under study and the room-temperature data are collected in Table 2. As expected, the fluorescence lifetimes decrease with increasing temperature owing to the increase in the rate constant of the reverse intersystem crossing from T₁ back to S₁ [see Eq. (4)]. The experimental

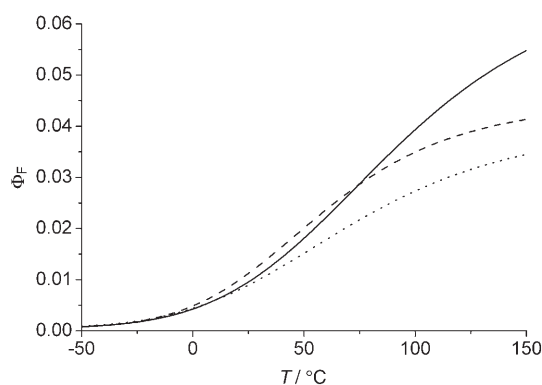


Figure 5. Fluorescence quantum yield versus temperature for C₇₀/PtBMA (solid line), C₇₀/PS (dashed line), and C₇₀-P1VN (dotted line).

data were fitted to Equation (4) (with ΔE_{ST} fixed at the value determined from the steady-state fit, Table 2). The τ_{DF} values for the C₇₀/PtBMA film as a function of temperature are shown in Figure 6. From the fit one obtains $A = 4.3 \times 10^7 \text{ s}^{-1}$ and $k_G^T = 29 \text{ s}^{-1}$, both parameters being in good agreement with previous determinations in liquid paraffin.^[21]

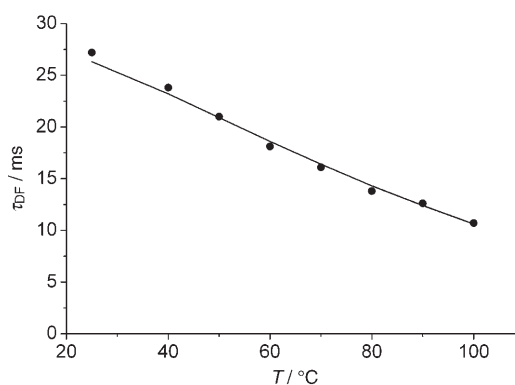


Figure 6. Temperature dependence of the experimental (circles) and calculated (solid line) fluorescence lifetimes (τ_{DF}) of C₇₀/PtBMA, with excitation at 470 nm and emission at 700 nm.

Temperature sensitivity of delayed fluorescence lifetime:

The relative sensitivity of the lifetime of the C₇₀/PtBMA system towards temperature is shown in Figure 7. The response covers a wide range, and the slope is quite steep. The temperature dependence of the lifetime of the [Ru(phen)]/PAN system^[31,32] is included for comparison.

Again, in order to estimate a working temperature range, a minimum value of 0.5% K⁻¹ for S_R was assumed. The results show a working temperature range of between 7°C (lifetime: 30 ms) and an estimated upper limit of 515°C (estimated lifetime: 175 μs). The estimated upper limit nevertheless only applies if the matrix remains solid as well as chemically and photophysically inert.

Temperature sensing using steady-state fluorescence: In measurements based on steady-state fluorescence intensities

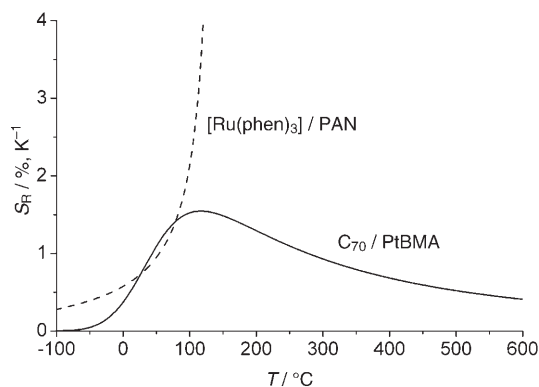


Figure 7. Relative sensitivity S_R of the fluorescence lifetime versus temperature for C_{70} /PtBMA (solid line) and for the $[Ru(phen)_3]$ /PAN standard (dashed line).

it is advantageous to use an internal standard. This is referred to as the ratiometric method. In our case, the standard to be incorporated into the C_{70} /PtBMA film must fulfil the following requirements: 1) A temperature-independent fluorescence quantum yield; 2) a fluorescence spectrum with no overlap with that of C_{70} ; 3) a common excitation wavelength with C_{70} . Perylene was chosen as a standard as its fluorescence intensity is temperature-independent in the film and temperature range used, its fluorescence spectrum does not overlap the C_{70} spectrum, and excitation can be made at 420 nm for both fluorophores. Perylene is also known for its high thermal stability.^[33] After addition of a very small amount of perylene (which suffices owing to its high Φ_F) to the film-forming mixture, fluorescence was excited at 420 nm and the emission spectra were recorded under the same conditions. Also, the ratios of I_F of perylene (recorded at 470 nm) and I_F of C_{70} (at 700 nm) were also computed. By using the same excitation wavelength (420 nm) it was possible to measure two independent fluorescence intensities (470 and 700 nm) derived from two different species, fullerene and the standard, and to relate their ratio to the temperature by means of a calibration curve. The temperature dependence of this data is shown in Figure 8. The line obtained is almost linear for temperatures between 25 and 70 °C.

C_{70} /PtBMA versus $[Ru(phen)_3]$ /PAN: Fluorescence intensity and lifetime imaging: The fluorescence intensity of C_{70} /PtBMA was also determined by steady-state fluorescence imaging. A similar system has been described previously^[34] and is based on a fast gateable monochrome charged-coupled device (CCD) camera and a number of pulsed light-emitting diodes (LEDs) as the light source. The light-encoded information is stored, pixel by pixel, in a grayscale format with background subtraction. Fluorescence intensity images of a C_{70} /PtBMA film in the absence of oxygen at different temperatures are shown in Figure 9.

In addition to intensity-based imaging, the rapid lifetime determination method (RLD)^[35] was applied to image the temperature dependence of the C_{70} /PtBMA system. In con-

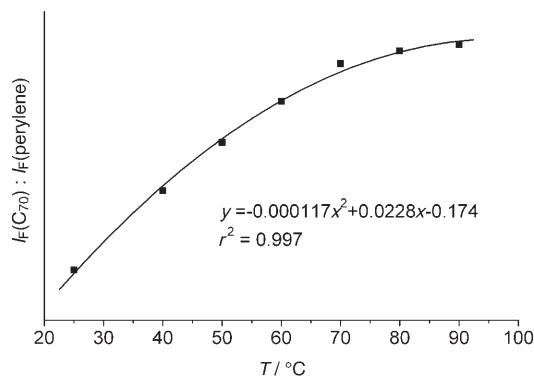


Figure 8. Temperature dependence of the ratio between I_F (700 nm) of C_{70} and I_F (470 nm) of perylene in PtBMA ($\lambda_{exc} = 420$ nm). The solid line corresponds to the nonlinear fit to the data, shown as black squares.

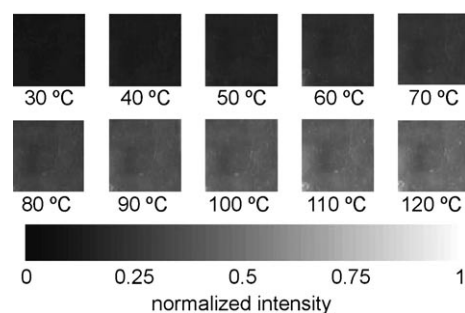


Figure 9. Steady-state fluorescence images of a C_{70} /PtBMA film at various temperatures.

trast to intensity-based imaging methods in which the quantification of a data matrix may be disturbed not only by a heterogeneous light field but also by a non-uniform distribution of the indicator within the planar sensing film, the intensity ratio G_1/G_2 is not affected in the RLD method. Figure 10 shows the results in pseudo-color code.

The lifetimes are similar to those presented in Figure 6. A strong temperature dependence is again observed with the lifetime decreasing with increasing temperature.

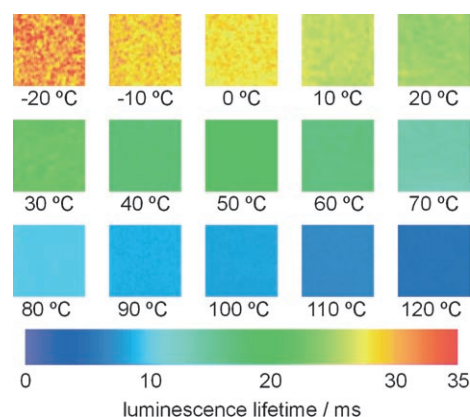


Figure 10. Fluorescence lifetime images of a C_{70} /PtBMA film at various temperatures.

The luminescence properties of ruthenium(II) polypyridyl complexes exhibit a strong temperature dependence. In particular, [Ru(phen)₃] (tris(1,10-phenanthroline)ruthenium) is a common optical temperature probe that displays efficient temperature quenching and high sensitivity. It is used because 1) it can be incorporated into solid matrices such as sol-gels or polymers; 2) it is commercially available; 3) it is photostable; 4) it has a large Stokes shift; 5) it can be excited in the visible region.^[31] However, the luminescence of Ru^{II} polypyridyl complexes is quenched by oxygen, and to avoid this interference in temperature sensing, poly(acrylonitrile) (PAN) was used as a matrix as a result of its very low gas permeability.^[36]

The temperature dependence of the luminescence quantum yields of C₇₀/PtBMA and [Ru(phen)₃]/PAN systems are shown in Figure 11. It can be seen that for temperatures higher than 80 °C the luminescence quantum yield of C₇₀ in PtBMA exceeds that of [Ru(phen)₃] in PAN.

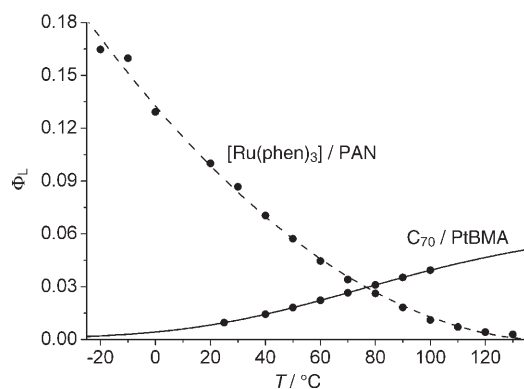


Figure 11. Temperature dependence of the luminescence quantum yields (Φ_L) of C₇₀/PtBMA (solid line) and [Ru(phen)₃]/PAN (dashed line). Experimental points are shown as circles.

The luminescence lifetimes of these two systems decrease with temperature. However, the lifetimes of the [Ru(phen)₃]/PAN system are always much shorter and its intensity continuously decreases with temperature. Above 110 °C the [Ru(phen)₃]/PAN system has a lifetime below 1 μs. Above 130 °C the intensities are too low for routine measurement. The temperature sensitivity of the lifetime of the [Ru(phen)₃]/PAN system is also shown in Figure 7.

The lifetime of C₇₀, on the other hand, is expected to remain in the hundreds of microseconds range at temperatures up to 500 °C (see Figure 7), and its intensity is expected to remain high above 130 °C (see Figure 5).

Conclusion

A study of the temperature dependence of the fluorescence intensity of C₇₀ in a solid polymer film has led to the development of a new type of optical molecular thermometer. Several polymers (PtBMA, P1VN, and PS) were tested.

With one of these (PtBMA), and under appropriate conditions (100 °C and the absence of oxygen), the fluorescence of C₇₀ increases by a factor of 79 relative to the fluorescence under aerated room-temperature conditions. Extrapolation of the results to higher temperatures allows the prediction of a maximum increase in the fluorescence of C₇₀ of two orders of magnitude (estimated maximum value of $\Phi_F = 0.071$) through thermally activated delayed fluorescence. We have determined the values of the effective singlet-triplet energy gap (ΔE_{ST}), the quantum yield of triplet formation (Φ_T), the fluorescence decay times (τ_{PF}) at room temperature, and the delayed fluorescence lifetimes (τ_{DF}) of the different systems. The C₇₀/PtBMA system exhibits the highest range of temperatures over which the relative variation exceeds 0.5 % K⁻¹ (-80 to 140 °C). The smaller range of sensitivity and the less favorable photophysical properties obtained with PS and P1VN are very likely due to π - π interactions between the fullerene and the phenyl rings of the backbone of the polymers, which are absent in PtBMA. The polymer films exhibit a high reversibility in heating/cooling temperatures cycles, and the results are reproducible. The C₇₀/PtBMA system was calibrated (and self-referenced) through the incorporation of perylene as an internal standard (perylene).

Note that visual perception of the usually very weak fluorescence of C₇₀ (and of all other pristine fullerenes) has not been reported previously. In the absence of oxygen and at temperatures above 20 °C, the red fluorescence of C₇₀ in the films is so intense that it is easily perceived by the naked eye. We present in this work (Figure 12) the first color pictures of the fluorescence of a fullerene.

The temperature dependence of the C₇₀/PtBMA system was compared with a film of [Ru(phen)₃] in PAN which is a common and well-documented optical temperature probe showing high sensitivity. Above 80 °C, the C₇₀/PtBMA system

displays fluorescence quantum yields higher than those of [Ru(phen)₃]/PAN and has much longer fluorescence lifetimes, estimated to remain in the hundreds of microseconds range at temperatures up to 500 °C. Work is in progress on the incorporation of C₇₀ into polymers with low oxygen permeability. Use of such media would obviate the need to degas the C₇₀ film. On the other hand, the extreme sensitivity of C₇₀ fluorescence intensity to molecular oxygen also makes its use advantageous in ultratrace oxygen sensing.^[37]

The C₇₀-based luminescence thermometer is a new development in the molecular thermometry field owing to the possibility of using a highly sensitive probe that covers not only both the low temperature and the physiological temperature ranges, but that can also be used for temperatures well above 100 °C.

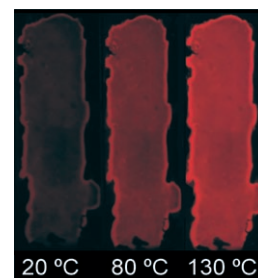


Figure 12. The first color pictures of the fluorescence of a fullerene.

Experimental Section

Materials: C_{70} (> 99.9%), polystyrene (PS, average $M_w \approx 280\,000$, pellets), poly(1-vinylnaphthalene) (P1VN, average $M_n \approx 100\,000$, powder), poly(*tert*-butyl methacrylate) (PtBMA, average $M_w \approx 170\,000$, crystals), tris(1,10-phenanthroline)ruthenium chloride hydrate and perylene were purchased from Aldrich (www.sigmaaldrich.com) and used as received. Toluene (Fluka, www.sigmaaldrich.com) and methyl cyclohexane (Aldrich, www.sigmaaldrich.com) were of spectroscopic grade. $[\text{Ru}(\text{phen})_3](\text{PF}_6)_2$ was synthesized according to the literature.^[31] Poly(acrylonitrile) (PAN, powder, average $M_w \approx 170\,000$) was purchased from Polyscience (www.polyscience.de). $[\text{Ru}(\text{phen})_3]$ in PAN was prepared following a literature procedure.^[8]

Preparation of the films: To prepare the fullerene-containing films, C_{70} (2.37 mmol) and the polymer (200 mg) were dissolved in toluene (2 mL) and a quartz plate was coated with the mixture at room temperature. In the case of the film that also incorporated perylene, C_{70} (2.37 mmol) and the polymer (200 mg) were dissolved in toluene (1 mL) and perylene in toluene (1 mL, 1×10^{-4} M) was added. The plate was introduced into a quartz cell and degassed at room temperature with a turbomolecular pump (final pressure: ca. 3×10^{-8} atm) and then the cell was sealed.

Spectral characterization: Absorption spectra of C_{70} in the polymer films in methylcyclohexane and in toluene were recorded with a UV-3101PC UV-Vis-NIR spectrophotometer (Shimadzu, www.shimadzu.com). Luminescence spectra were obtained with a Fluorolog F112A fluorimeter (Spex, www.jobinyvon.com) in a front-face configuration. The excitation wavelength was 470 nm and the excitation and emission slits were 18 and 9 nm, respectively. The sample film was mounted slightly away from a 45° angle to minimize specular reflection of the excitation light. Emission spectra were not corrected for the spectral response of the optics and photomultiplier. The temperature was controlled to within $\pm 0.5^\circ\text{C}$. Time-resolved picosecond fluorescence intensity decays were obtained by the single-photon timing method with laser excitation, with excitation at 470 nm and emission at 700 nm. The set up consisted of a mode-locked Innova 400-10 argon ion laser (Coherent, www.cohr.com) that synchronously pumped a cavity-dumped 701-2 dye laser (Coherent, www.cohr.com), delivering 3–4 ps pulses (with ca. 40 nJ pulse^{-1}) at a frequency of 3.4 MHz. Intensity decay measurements were made by alternated collection of impulse and decays with the emission polarizer set at the magic-angle position. Impulses were recorded slightly away from the excitation wavelength with a scattering suspension. For the decays, a cut-off filter was used to effectively remove excitation light. Detection was always performed by passing the emission through a depolarizer and then through a HR320 monochromator (Jobin-Yvon, www.jobinyvon.com) with a grating of 100 lines mm^{-1} . Usually no less than 5000 counts were accumulated at the maximum channel. A 2809U-01 microchannel plate photomultiplier (Hamamatsu, www.hamamatsu.com) served as the detector. Its response function had an effective FWHM of 35 ps.^[38] Decay data analysis was performed with the Globals Unlimited software package.^[39]

Imaging of C_{70} and $[\text{Ru}(\text{phen})_3]$: All measurements were carried out in a self-developed custom flow chamber. It was connected to a RC6 Thermostat from Lauda (www.lauda.com) which ran on silicon oil M 10 from Roth (www.roth.de). The gas flow in the cell was adjusted by two PR 4000 pressure controllers (MKS Instruments, www.mksinst.com). The gases used were nitrogen (purity 5.0) and synthetic air, both from Linde (www.linde.com). Both dyes were excited by using four Luxeon V Star LXHL-LB5C LEDs (Lumileds Lighting, www.lumileds.com). This LED has a brightness of 30 Lm and a center emission of 470 nm. The excitation light was focused by PCX 18 × 18 MgF2 TS lenses (Edmund Optics, www.edmundoptics.com) and was directed onto the sensor at an angle of approximately 20°. It was filtered through a FITCA filter (Schott, www.schott.de). Emission was recorded through a Chroma 680 filter for fullerene and a Chroma 580 filter for the ruthenium complex; both filters have a FWHM of around 60 nm (AHF Analysentechnik, www.ahf.de). Steady-state and fluorescence lifetime images were acquired using a modulated CCD camera (Imagex TG1, Photonic Research, www.prsbio.com) equipped with a Xenon 0.95/17 mm lens (Schneider, www.schneideroptics.com). The rapid lifetime determination (RLD) method^[35] was

used to calculate the luminescence lifetimes. Following a square-shaped light pulse, luminescence was detected quantitatively in two different gates. The first gate (G_1) was only opened after a period of 1 μs after switching off the LEDs to avoid short-lived background fluorescence. Potential interferences caused by backscattered excitation light were also eliminated in this manner. The second gate (G_2) was opened immediately after the closure of G_1 . The ratio G_1/G_2 is virtually independent of the overall signal intensity. Assuming a monoexponential decay and a constant aperture time for each gate, the decay time τ of each pixel can be calculated as $\tau = \Delta t / \ln(G_1/G_2)$, where Δt is the integration time and G_1 and G_2 are the areas of each gate.

Acknowledgements

This work was supported by the Fundação para a Ciência e a Tecnologia (FCT, Portugal) and POCI 2010 (FEDER) within project POCI/QUI/58535/2004. C.B. was supported by a postdoctoral fellowship from the FCT (SFRH/BPD/14561/2003).

- [1] R. Narayanaswamy, O. S. Wolfbeis, *Optical Sensors for Industrial, Environmental and Clinical Applications*, Springer, Berlin, **2004**.
- [2] O. S. Wolfbeis, *Anal. Chem.* **2004**, *76*, 3269–3284.
- [3] O. S. Wolfbeis, *Anal. Chem.* **2006**, *78*, 3859–3874.
- [4] K. T. Grattan, Z. Y. Zhang, *Fiber Optic Fluorescence Thermometry*, Chapman and Hall, London, **1995**.
- [5] J. N. Demas, B. A. DeGraff, *Proc. SPIE-Int. Soc. Opt. Eng.* **1992**, *1796*, 71–75.
- [6] S. A. Wade, S. F. Collins, G. W. Baxter, *J. Appl. Phys.* **2003**, *94*, 4743–4756.
- [7] S. Uchiyama, A. P. de Silva, K. Iwaw, *J. Chem. Educ.* **2006**, *83*, 720–727.
- [8] J. N. Demas, B. A. DeGraff, *Coord. Chem. Rev.* **2001**, *211*, 317–351.
- [9] N. Chandrasekharan, L. A. Kelly in *Reviews in Fluorescence 2004* (Eds.: C. D. Geddes, J. R. Lakowicz), Kluwer Academic, New York, **2004**, pp. 21–40.
- [10] B. Valeur, *Molecular Fluorescence: Principles and Applications*, Wiley-VCH, Weinheim, **2002**.
- [11] M. W. Wolf, K. D. Legg, R. E. Brown, L. A. Singer, J. H. Parks, *J. Am. Chem. Soc.* **1975**, *97*, 4490–4497.
- [12] A. M. Turek, G. Krishnamoorthy, K. Phipps, J. Saltiel, *J. Phys. Chem. A* **2002**, *106*, 6044–6052.
- [13] A. Maciejewski, M. Szymanski, R. P. Steer, *J. Phys. Chem.* **1986**, *90*, 6314–6318.
- [14] J. L. Kropp, W. R. Dawson, *J. Phys. Chem.* **1967**, *71*, 4499–4506.
- [15] B. Nickel, D. Klemp, *Chem. Phys.* **1993**, *174*, 297–318.
- [16] B. Nickel, D. Klemp, *Chem. Phys.* **1993**, *174*, 319–330.
- [17] J. C. Fister III, D. Rank, J. M. Harris, *Anal. Chem.* **1995**, *67*, 4269–4275.
- [18] J. W. Arbogast, C. S. Foote, *J. Am. Chem. Soc.* **1991**, *113*, 8886–8889.
- [19] S. M. Argentine, K. T. Kotz, A. H. Francis, *J. Am. Chem. Soc.* **1995**, *117*, 11762–11767.
- [20] M. R. Wasielewski, M. P. O’Neil, K. R. Lykke, M. J. Pellin, D. M. Gruen, *J. Am. Chem. Soc.* **1991**, *113*, 2774–2776.
- [21] M. N. Berberan-Santos, J. M. M. Garcia, *J. Am. Chem. Soc.* **1996**, *118*, 9391–9394.
- [22] S. M. Bachilo, A. F. Benedetto, R. B. Weisman, J. R. Nossal, W. E. Billups, *J. Phys. Chem. A* **2000**, *104*, 11265–11269.
- [23] F. A. Salazar, A. Fedorov, M. N. Berberan-Santos, *Chem. Phys. Lett.* **1997**, *271*, 361–366.
- [24] B. Gigante, C. Santos, T. Fonseca, M. J. M. Curto, H. Luftmann, K. Bergander, M. N. Berberan-Santos, *Tetrahedron* **1999**, *55*, 6175–6182.
- [25] S. M. Anthony, S. M. Bachilo, R. B. Weisman, *J. Phys. Chem. A* **2003**, *107*, 10674–10679.

- [26] Preliminary results were presented at the 9th *International Conference on Methods and Applications of Fluorescence* (MAF 9, Lisbon, 2005) and published in the MAF 9 conference proceedings. See also: C. Baleizão, M. N. Berberan-Santos, *J. Fluoresc.* **2006**, *16*, 215–219.
- [27] C. A. Parker, *Photoluminescence of Solutions*, Elsevier, Amsterdam, **1968**.
- [28] F. Tanaka, M. Okamoto, S. Hirayama, *J. Phys. Chem.* **1995**, *99*, 525–530.
- [29] M. Rae, M. N. Berberan-Santos, *Chem. Phys.* **2002**, *280*, 283–293.
- [30] G. Sarova, M. N. Berberan-Santos, *J. Phys. Chem. B* **2004**, *108*, 17261–17268.
- [31] G. Liebsch, I. Klimant, O. S. Wolfbeis, *Adv. Mater.* **1999**, *11*, 1296–1299.
- [32] S. M. Borisov, A. S. Vasylevska, C. Krause, O. S. Wolfbeis, *Adv. Funct. Mater.* **2006**, *16*, 1536–1542.
- [33] A. J. Bur, M. G. Vangel, S. Roth, *Appl. Spectrosc.* **2002**, *56*, 174–181.
- [34] G. Liebsch, I. Klimant, C. Krause, O. S. Wolfbeis, *Anal. Chem.* **2001**, *73*, 4354–4363.
- [35] G. Liebsch, I. Klimant, B. Frank, G. Holst, O. S. Wolfbeis, *Appl. Spectrosc.* **2000**, *54*, 548–559.
- [36] J. Brandrup, E. H. Immergut, E. A. Grulke, *Polymer Handbook*, Wiley, New York, **1999**.
- [37] S. Nagl, C. Baleizão, S. M. Borisov, M. Schäferling, M. N. Berberan-Santos, O. S. Wolfbeis, *Angew. Chem. Int. Ed.* **2007**, *46*, in press.
- [38] A. A. Fedorov, S. P. Barbosa, M. N. Berberan-Santos, *Chem. Phys. Lett.* **2006**, *421*, 157–160.
- [39] Globals Unlimited, Laboratory for Fluorescence Dynamics, University of Illinois (USA).

Received: November 5, 2006
Published online: February 7, 2007